Tailoring the electrical properties of MoS₂ field effect transistors by depositing Au nanoparticles and alkanethiol molecules

Kyungjune Cho, Hyunhak Jeong, Tae-Young Kim, Jinsu Pak, Jae-Keun Kim, Barbara Yuri Choi and Takhee Lee

Department of Physics and Astronomy, and Institute of Applied Physics, Seoul National University, Seoul 08826, Korea

E-mail: tlee@snu.ac.kr

CrossMark

Abstract

We fabricated and characterized MoS₂ field effect transistors. First, we measured the electrical properties of MoS₂ field effect transistors (FETs) that were made with mechanically exfoliated MoS₂ flakes. Then, we deposited Au nanoparticles on the MoS₂ channel and measured the electrical properties. We observed whether the source-drain current increased or decreased after the Au particles were deposited. The deposited Au particles either formed an extra current path and increased the current or behaved as charge-withdrawing sites and decreased the current. Next, we deposited alkanethiol molecules on the Au particles to reduce the work function of the Au. Alkanethiol molecules are known to form a self-assembled monolayer on the Au surface, and the electric dipole moment of the molecules causes the work function of the Au to decrease. Au particles can capture electrons from the MoS₂ channel due to their high work function. However, the decreased work function of the Au particles subjected to alkanethiol treatment could cause captured electrons to be released from the Au particles to MoS₂. Therefore, the current increased after alkanethiol treatment. This study may provide useful methods to utilize surface treatments with particles and molecules to tailor the electrical properties of MoS₂-based FETs.

(Some figures may appear in colour only in the online journal)

1. Introduction

Two-dimensional (2D) transition metal dichalcogenides (TMD) that have an atomic layered structure have drawn significant attention as promising ultra-thin semiconductors. Graphene, single carbon atomic layer, which is a representative 2D layered material, has distinct limitations in that it does not have a band gap for use as a semiconductor or it has only a small band gap at best [1–3]. However, it has several other advantageous features as a 2D layered material, such as a high electric carrier mobility, optical transparency, and good mechanical properties [4, 5]. In contrast, TMD family materials have a finite band gap for use as semiconductors [6, 7]. TMD materials also have favorable physical characteristics, such as good flexibility, reasonable mobility, high transparency, and the availability of complex device structures due to their low-dimensional structure [7]. Molybdenum disulfide (MoS₂), which is a TMD material, has been actively studied because of these advantages. MoS₂ behaves as an n-type semiconductor and is well known to have a direct electric band gap of ~1.9 eV as a single-layer MoS₂ and an indirect one of ~1.2 eV as a bulk MoS₂ crystal [8, 9]. Single-layer MoS₂ also has good electrical properties, such as a high carrier mobility (~tens of cm² Vs⁻¹ or more) and a high current on/off ratio

(~10^5 or more). These excellent properties enable the use of MoS$_2$ in transistors, memory, logic circuits, and sensor devices [10–18].

Although MoS$_2$ already has good physical properties, controlling its electrical properties is important for its application. The surface treatment of MoS$_2$ channels can be an efficient method for this purpose [19, 20]. In this study, we fabricated and characterized MoS$_2$ field effect transistors (FETs) with mechanically exfoliated MoS$_2$ flakes. Then, we deposited Au nanoparticles on the MoS$_2$ FETs and investigated how the deposited Au particles influenced their electrical properties. We then deposited alkanethiol (HS(CH$_2$)$_{n-1}$CH$_3$) molecules on the Au particle surfaces. The alkanethiol molecule, which has an aligned electric dipole moment, can change the work function of Au by forming a self-assembled monolayer on the Au surface [21–24]. We applied the alkanethiol molecule to the Au particle-deposited MoS$_2$ FETs and investigated the electrical properties. We compared the electrical properties of MoS$_2$ FETs both before and after the Au particle deposition and before and after the alkanethiol treatment.

2. Experimental details

2.A. Device fabrication procedure

We fabricated five different MoS$_2$ FET devices. First, we prepared a SiO$_2$/Si substrate with a heavily p-doped Si layer for use as a back gate. We transferred MoS$_2$ flakes onto the SiO$_2$ layer (270 nm) of the substrate from a bulk MoS$_2$ crystal by using a micromechanical exfoliation method. Then, using an optical microscope, we located MoS$_2$ flakes that were suitable for fabricating the FET devices. Subsequently, we measured the height of those flakes using an atomic force microscope (AFM) system. We spin-coated a buffer layer polymer (MMA (8.5) MAA (9% concentration in ethyl lactate)) and an electron resist polymer (PMMA 950K (5% concentration in anisole)) to prepare electrode patterns using an electron-beam lithography system. After the spin-coating process, we prepared source and drain electrode patterns. Finally, we deposited 5-nm-thick Ti and 50 nm-thick Au as electrodes using an electron-beam evaporator.

2.B. Detailed experimental process

Figure 1(a) represents the schematic of the experimental process. First, we fabricated an MoS$_2$ FET device (Top). Then, we measured the electrical properties of the MoS$_2$ FETs using a semiconductor parameter analyzer (Keithley 4200-SCS). The electrical measurements were done at a temperature-variable probe station (JANIS Model ST-500) under vacuum conditions to prevent unwanted effects from oxygen and water. After the electrical measurements were taken, we deposited very thin Au (less than 1 nm thick) to prepare an Au particle structure on the MoS$_2$ surface, as shown in the middle image of figure 1(a). With the small thickness of the Au film, we could prepare Au particles on the MoS$_2$ surface. After the deposition, we measured the electrical properties of the MoS$_2$ FETs again and compared the data before and after the Au

particle deposition. We then applied an alkanethiol molecule treatment to the devices. In this study, we used hexadecanethiol (HS(CH$_2$)$_{15}$CH$_3$) molecules, which have 16 carbons in the alkane chain. The alkanethiol molecules tend to form a self-assembled monolayer (SAM) on the Au surface, as shown in the bottom of figure 1(a). We dipped the devices in a 5 mM hexadecanethiol solution for 15 h to form alkanethiol SAMs on the Au particles. These molecules, which have an aligned electric dipole moment, cause the work function of Au to decrease. We measured and compared the electrical properties of the devices before and after the alkanethiol molecule treatment.

Figure 1(b) shows the optical image and AFM image of one of the fabricated devices. Figure 1(c) displays the AFM images of the surface of MoS$_2$ before and after the Au particle formation. When we deposited Au to prepare a particle-like structure, the substrate was rotating in the electron-beam evaporator system, and the Au was deposited with a high evaporation rate (~1 Å s^{-1}). For these reasons, the Au particles could have an oval shape aligned in a random particular direction, as shown in the image of 'After' Au deposition in figure 1(c).

3. Results and discussion

We measured the output characteristics and transfer characteristics of the MoS$_2$ FET devices. Figure 2(a) shows the output curves (source-drain current versus source-drain voltage, I_{DS}–V_{DS}) of one of the devices with various gate voltages from −30 to 30 V with a step of 10 V. Figure 2(b) displays the transfer curve (source-drain current versus gate voltage, I_{DS}–V_G) of the same device with a fixed source-drain voltage of 0.5 V. The inset of figure 2(b) shows the transfer curve with a logarithmic current scale. The MoS$_2$ devices exhibit typical *n*-type behavior, as is known. The threshold voltage (V_{Th}) was found to be −28.6 V, and the field effect mobility was found to be 11.5 cm^2 Vs^{-1} for the data of figure 2(b). We determined the V_{Th} from V_G-axis intercept obtained from the linear fitting of the V_G–I_D curves and the field effect mobility was calculated by using following formula, $\mu = \left[\frac{dI_{DS}}{dV_G}\right] \times \left[\frac{L}{(WC_iV_{DS})}\right]$ where W is the channel width, L is the channel length and C_i is the capacitance per area between channel and gate.

Then, we deposited Au particles on MoS$_2$ FET devices, as explained in the Experimental section, and we measured the electrical characteristics of the Au-particle deposited MoS$_2$ FETs. Figure 3 shows the transfer characteristics of MoS$_2$ FETs before and after the Au particle deposition and alkanethiol SAM treatment. Figure 3 shows that the representative electrical data of each case which were measured from different devices. The black curves in figure 3 were measured before the Au particle deposition, and the blue curves in figure 3 were measured after the Au particle deposition. We observed that the source-drain current increased (figures 3(a) and (b)) or decreased (figure 3(d) and (e)) after the Au particle deposition. Note that the devices may be affected by O$_2$ or water vapor while they are exposed to ambient during a series of treatments. O$_2$ and water vapor capture the electrons
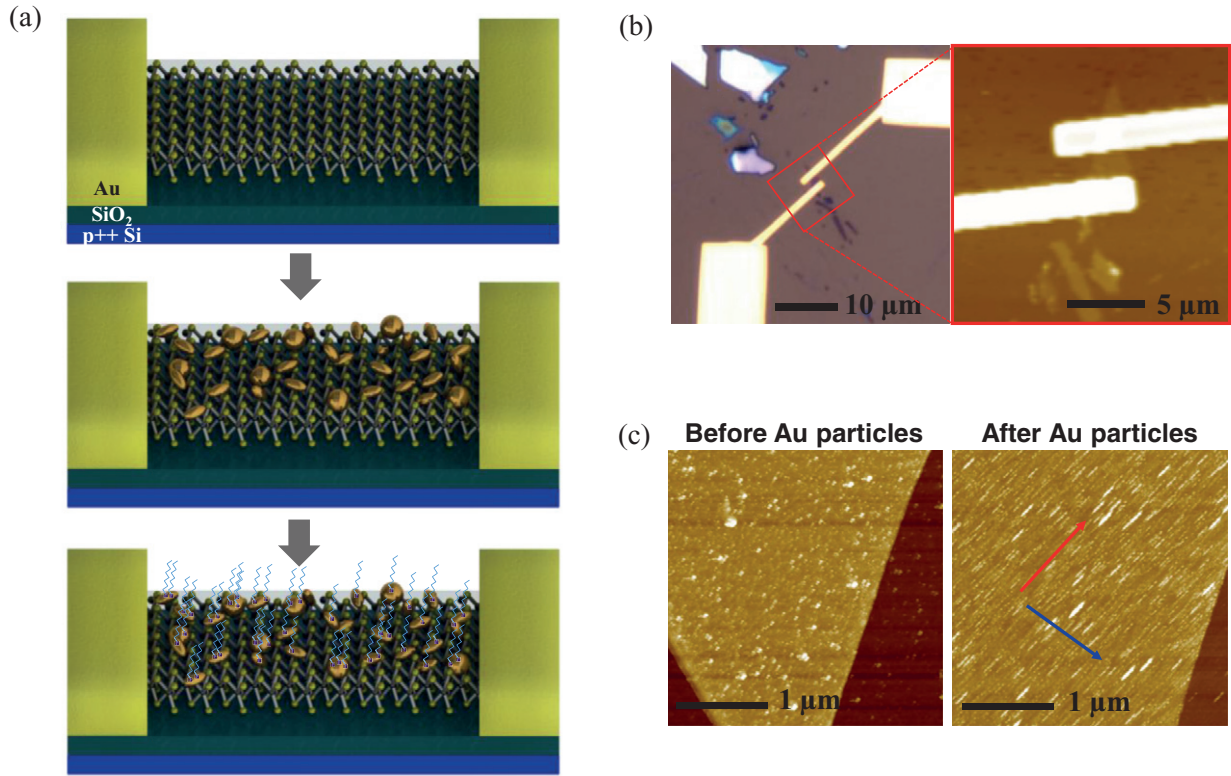
Figure 1. (a) Schematic images of experimental process. (b) Optical image (left) and AFM image (right) of a fabricated device. (c) AFM image of MoS_2 flake before and after Au particle deposition. Note that the Au particles are not scaled in (a).
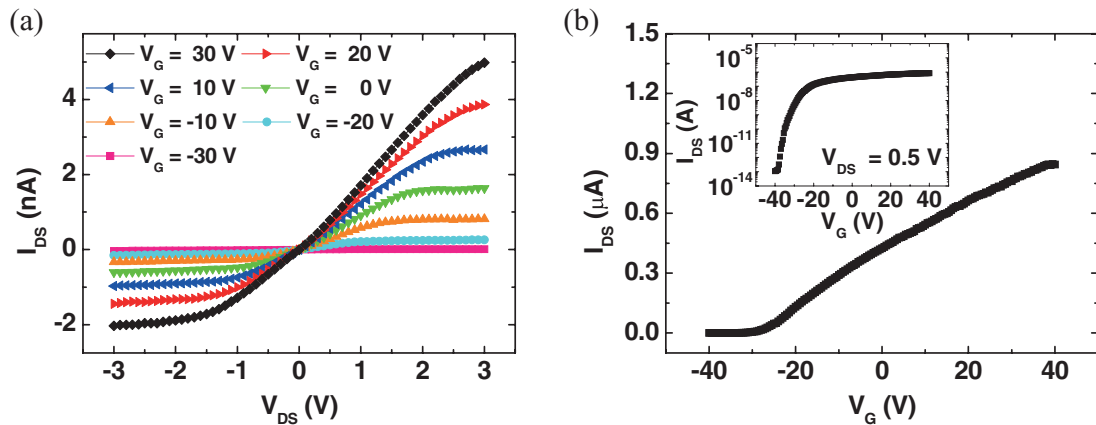

Figure 2. (a) I_{DS}–V_{DS} curves measured with various gate voltages from −30 to 30 V. (b) I_{DS}–V_G curve measured at a fixed $V_{DS} = 0.5$ V. The inset shows the I_{DS}–V_G curve with a logarithmic scale.

from MoS_2 channel and cause the source-drain current of the devices to decrease only, but not to increase [25, 26]. Therefore, we think these environmental effects are not dominant in this study. Schematic images explaining the observed phenomena are shown in the right side of figure 3. As one can see in figure 1(c), the oval shaped Au particles were aligned in a particular direction. If the Au particles are aligned along the channel direction (indicated by a red line in the figure 3(c) and in figure 1(c)), the Au particles can behave as additional current paths on the channel surface of MoS_2 because of the high conductance of Au. In this case, the source-drain current level increases with the Au particle deposition (see the curves

labelled 'Pristine' and 'Au (as current path)' before and after the Au particle deposition, respectively, in figure 3(a)). In contrast, if the particles are aligned perpendicularly to the channel direction (blue lines in the figure 3(f) and in figure 1(c)), the Au particles may behave as charge-withdrawing sites because of the high work function of Au. In this case, the deposited Au particles that have a higher work function than MoS_2 cause electrons to transfer from MoS_2 to the Au particles. Therefore, the source-drain current level decreased after the Au particle deposition (see the curves labelled 'Pristine' and 'Au (as charge-withdrawing)' before and after the Au particle deposition, respectively, in figure 3(d)). If the deposited Au formed
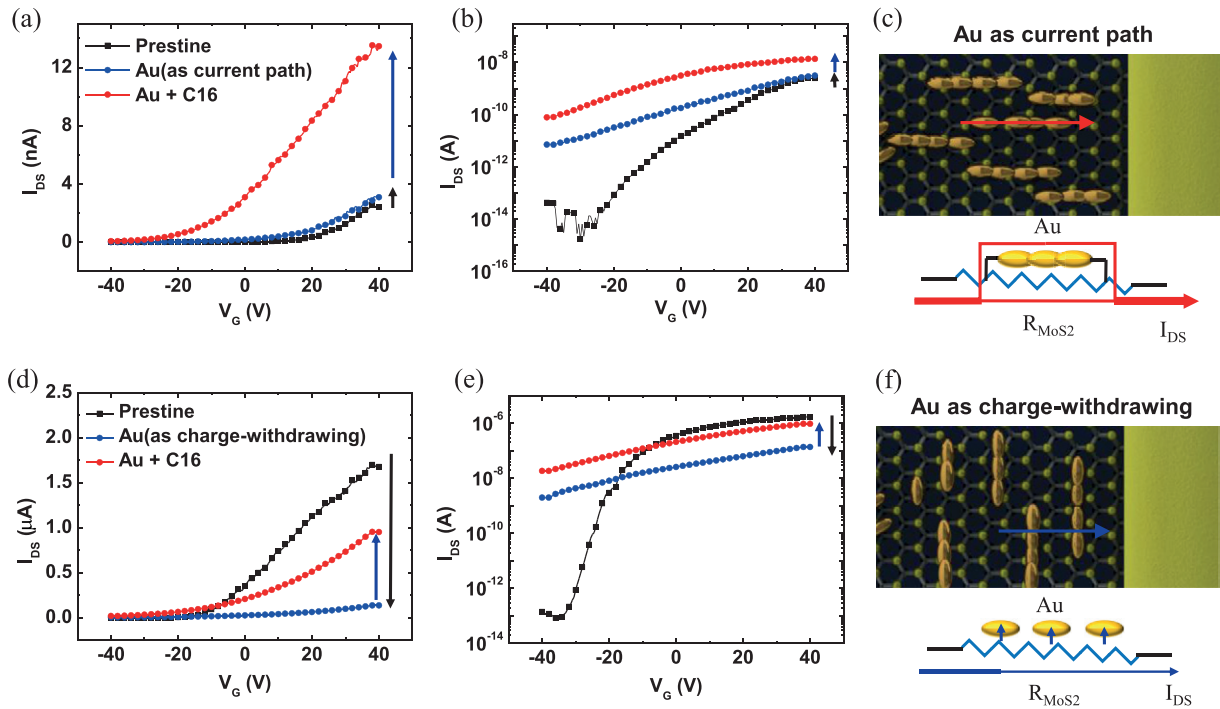
Figure 3. I_{DS}–V_G curves with linear (a) and logarithmic scales (b) measured before and after the Au particle deposition and after the alkanethiol molecule treatment for the case when Au particles behave as an additional current path. The schematic images (c) explain that the Au particles behave as current paths. I_{DS}–V_G curves with linear (d) and logarithmic scales (e) measured before and after the Au particle deposition and after the alkanethiol molecule treatment for the case when the Au particles behave as charge-withdrawing sites. The schematic images (f) explain that the Au particles behave as charge-withdrawing sites. Note that the Au particles are not scaled in the schematics.
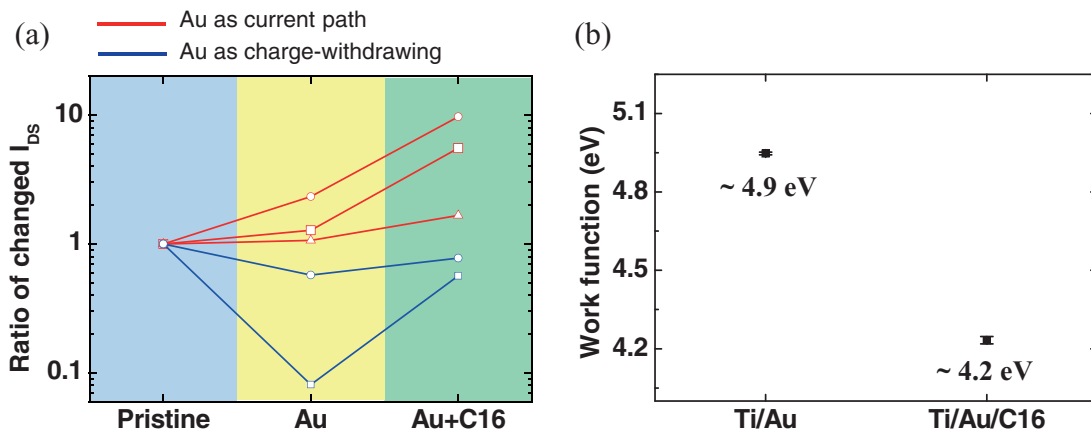

Figure 4. (a) Ratios of changed I_{DS} before and after Au particle deposition and after the alkanethiol molecule treatment. (b) Work function of Ti/Au film before and after alkanethiol molecule treatment.

connecting film, the source-drain current only had decreased, rather than increased or decreased. Therefore, we could know that the Au particles were formed after Au deposition.

Then, we applied hexadecanethiol (denoted as C16) molecules to the Au-deposited MoS$_2$ FET devices, as explained in the experimental section. The molecules with thiol end groups tend to form a self-assembled monolayer on the Au surface [21–24]. Because alkanethiol molecules have an electrical dipole moment (the dipole direction is from the thiol to the CH$_3$ end), they cause the work function of Au to decrease. Therefore, electrons tend to be released from the Au particles to MoS$_2$ as a result of the alkanethiol molecule treatment.

This causes the source-drain current to increase, as shown in figure 3 (see the curves labelled 'Au + C16' in figure 3(a) and (d)). The current increased after the alkanethiol molecule treatment for both cases of Au particles (Au particles as current path or charge-withdrawing sites).

In this study, we systemically studied the effects of Au particle deposition and alkanethiol treatment with 5 different devices. Figure 4(a) summarizes the ratios of the source-drain currents of the 5 MoS$_2$ FET devices for each case (before and after the Au particle deposition and alkanethiol molecule treatment) at same gate voltage and source-drain voltage. Here, the current before any treatment was set to 1, and the
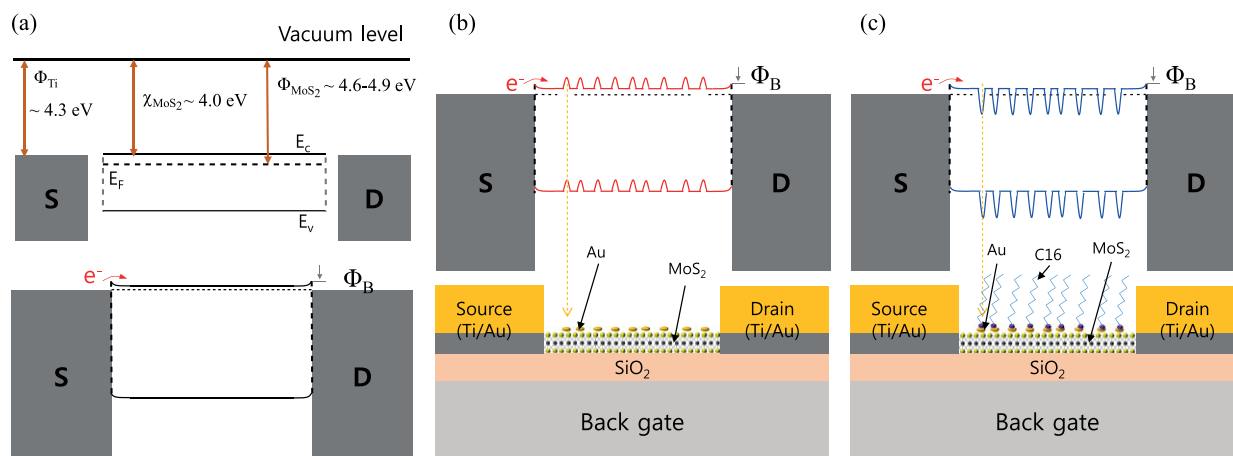
Figure 5. (a) Schematics of the energy band diagrams at $V_G = 0$ V before and (b) after Au particle deposition and (c) after the alkanethiol molecule treatment.

ratios of the changed currents were plotted. The red data represent the case when the deposited Au particles behave as a current path on the MoS$_2$ surface, and the blue data represent the other case, i.e. when the deposited Au particles behave as charge-withdrawing sites on the MoS$_2$ surface. To confirm that the alkanethiol molecule decreases the work function of Au, we measured the work function of an Au(30 nm)/Ti(5 nm) film using a Kelvin probe force microscope system before and after the alkanethiol molecule treatment. The work function of the film was found to be ~4.9 eV and ~4.2 eV before and after the molecule treatment, respectively (figure 4(b)). The alkanethiol substantially decreased the work function of Au. Then, the thiol molecule-deposited Au particles release electrons from Au to MoS$_2$, thus causing the current to increase after the treatment (see figures 3 and 4).

We now explain the observed phenomena in terms of energy band diagrams. Figure 5 shows the energy band diagrams of the MoS$_2$ active channel between the Ti source (*S*) and drain (*D*) electrodes. Figure 5(a) displays the energy level of the MoS$_2$ channel and Ti electrodes. The MoS$_2$ channel used in this study has a band gap energy of ~1.4 eV, a work function (Φ_{MoS2}) of 4.6–4.9 eV, and an electron affinity (χ_{MoS2}) of ~4.0 eV. We used Ti/Au as source-drain electrodes that contact with MoS$_2$. Ti layer with 5 nm-thick was used as an adhesion layer between Au and MoS$_2$ contact. Although the work function of Ti (~4.3 eV) is lower than the work function of MoS$_2$ (4.6–4.9 eV), a small Schottky barrier is formed between Ti and MoS$_2$ contact, as indicated in figure 5(a) due to structural defect of MoS$_2$ [27–29]. Figure 5(b) displays the energy band diagram after the Au particle deposition. After the Au particle deposition, electrons transfer from MoS$_2$ to the Au particles due to the work function difference. This can be depicted as a depletion barrier at the MoS$_2$ channel, and these barriers cause the source-drain current to decrease. Figure 5(c) displays the energy band diagram after the alkanethiol molecule treatment. After the molecules adhere to the surface of the Au particles, they decrease the work function of the Au. Therefore, the electrons tend to be released from the Au particles to MoS$_2$, and as a result, the current increases after the alkanethiol molecule treatment.

4. Summary and conclusions

In summary, we fabricated MoS$_2$-based field effect transistors and measured their electrical characteristics. We deposited oval-shaped Au particles on the MoS$_2$ channel. The Au particles formed an additional current path that increases the source-drain current or withdrawing electrons from the MoS$_2$ channel and decreases the current compared with the MoS$_2$ FETs prior to the Au particle deposition. Then, we applied alkanethiol molecules onto the Au particle-deposited MoS$_2$. The alkanethiol molecules formed self-assembled monolayers on the Au surface and reduce the work function of the Au, which caused electrons to be released from the Au particles to the MoS$_2$ channel. Therefore, the source-drain current increased after the alkanethiol molecule treatment. Our study may provide insight into the usefulness of the surface treatment of particles or molecules on MoS$_2$-based nanoelectronic devices.

Acknowledgments

References

[1] Li X, Wang X, Zhang L, Lee S and Dai H 2008 *Science* **319** 1229
[2] Allen M J, Tung V C, and Kanar R B 2010 *Chem. Rev.* **110** 132
[3] Xu Y, Bai H, Lu G, Li C and Shi G 2008 *J. Am. Chem. Soc.* **130** 5856
[4] Novoselov K, Geim A K, Morozov S, Jiang D, Zhang Y, Dubonos S, Grigorieva I and Firsov A 2004 *Science* **306** 666
[5] Novoselov K, Jiang D, Schedin F, Booth T J, Khotkevich V V, Morozov S V and Geim A K 2005 *Proc. Natl. Acad. Sci. USA* **102** 10451
[6] Fang H, Chuang S, Chang T C, Takei K, Takahashi T and Javey A 2012 *Nano Lett.* **12** 3788

 [7] Radisavljevic B, Radenovic A, Brivio J, Giacometti V and
Kis A 2011 *Nat. Nanotechnol.* **6** 147
 [8] Kam K and Parkinson B 1982 *J. Phys. Chem.* **86** 463
 [9] Mak K F, Lee C, Hone J, Shan J and Heinz T F 2010 *Phys.
Rev. Lett.* **105** 136805
[10] Perkins F K, Friedman A L, Cobas E, Campbell P M,
Jernigan G G and Jonker B T 2013 *Nano Lett.* **13** 668
[11] Jariwala D, Sangwan V K, Lauhon L J, Marks T J and
Hersam M C 2014 *ACS Nano* **8** 1102
[12] Lee H S, Min S W, Park M K, Lee Y T, Jeon P J, Kim J H,
Ryu S and Im S 2012 *Small* **8** 3111
[13] Yin Z, Zeng Z, Liu J, He Q, Chen P and Zhang H 2013 *Small*
9 727
[14] Wang H, Yu L, Lee Y H, Shi Y, Hsu A, Chin M L, Li L J,
Dubey M, Kong J and Palacios T 2012 *Nano Lett.* **12** 4674
[15] Radisavljevic B, Whitwick M B and Kis A 2011 *ACS Nano*
5 9934
[16] Choi W *et al* 2012 *Adv. Mater.* **24** 5832
[17] Kim S *et al* 2012 *Nat. Commun.* **3** 1011
[18] Li H, Yin Z, He Q, Li H, Huang X, Lu G, Fam D W H,
Tok A I Y, Zhang Q and Zhang H 2012 *Small* **8** 63

[19] Najmaei S *et al* 2014 *Nano Lett.* **14** 1354
[20] Cho K, Min M, Kim T-Y, Jeong H, Pak J, Kim J-K, Jang J,
Yun S J, Lee Y H, Hong W-K and Lee T 2015 *ACS Nano*
9 8044
[21] Heimel G, Romaner L, Bredas J L and Zoger E 2006 *Phys
Rev. Lett.* **96** 196806
[22] Love J C, Estroff L A, Kriebel J K, Nuzzo R G and
Whitesides G M 2005 *Chem. Rev.* **105** 1103
[23] Boer B, Hadipour A, Mandoc M M, Woudenbergh T and
Blom P W M 2005 *Adv. Mater.* **17** 621
[24] Zangmeister C D, Picraux L B, Zee R D, Yao Y and Tour J M
2007 *Chem. Phys. Lett.* **442** 390
[25] Cho K, Park W, Park J, Jeong H, Jang J, Kim T-Y, Hong W-K,
Hong W and Lee T 2013 *ACS Nano* **7** 7751
[26] Park W, Park J, Jang J, Lee H, Jeong H, Cho K, Hong S and
Lee T 2013 *Nanotechnology* **24** 095202
[27] Feng L P, Su J and Liu Z T 2014 *J. Alloy. Compd.* **613** 122
[28] Kang J, Lue W and Banerjee K 2014 *Appl. Phys. Lett*
104 233502
[29] Feng L P, Su K, Li D P and Liu Z T 2015 *Phys. Chem. Chem.
Phys.* **17** 6700